

Good Time to Ask: A Learning Framework for Asking for Help in Embodied Visual Navigation

Jenny Zhang

Institute for Infocomm Research, A*STAR
jenny_zhang@i2r.a-star.edu.sg

Samson Yu

Centre for Frontier AI Research, A*STAR
samson_yu@ihpc.a-star.edu.sg

Jiafei Duan

Institute for Infocomm Research, A*STAR
duan_jiafei@i2r.a-star.edu.sg

Cheston Tan

Centre for Frontier AI Research, A*STAR
cheston-tan@i2r.a-star.edu.sg

Abstract: In reality, it is often more efficient to ask for help than to search the entire space to find an object with an unknown location. We present a learning framework that enables an agent to actively ask for help in such embodied visual navigation tasks, where the feedback informs the agent of where the goal is in its view. To emulate the real-world scenario that a teacher may not always be present, we propose a training curriculum where feedback is not always available. We formulate an uncertainty measure of where the goal is and use empirical results to show that through this approach, the agent learns to ask for help effectively while remaining robust when feedback is not available.

Keywords: Embodied AI, Human-Robot Interaction, Visual Navigation

1 Introduction

Consider the following scenario: you instruct a newly deployed robot assistant to retrieve a tool for you, but the robot does not know its location. Hence, it searches your entire home for it. It would be far more efficient if it could ask someone familiar with the task and environment for help, as shown in Figure 1. We naturally want to seek assistance when a task is difficult. This is especially the case when we lack sufficient information about the goal and/or the environment. Similarly, robots should be endowed with the ability to actively query and gain relevant knowledge to be more efficient and effective. However, robots in many robotics works [1, 2, 3, 4, 5, 6] do not have access to external assistance when tackling their navigation tasks.

We propose **Good Time to Ask (GTA)**, a learning framework to train and evaluate an embodied agent with the added capability of asking for feedback. We set the task to be object-goal navigation (ObjectNav) in AI2-THOR [7], an embodied AI [8, 9] simulator with a photorealistic indoor environment. We employ an interactive reinforcement learning (IRL) approach in training our agent to learn to seek help in the form: “Is the target object in view?”. To evaluate the quality of a query by the agent in the ObjectNav task, we present two important considerations:

- *Timing* - When is the best time for the agent to ask for assistance?
- *Robustness* - How do we prevent the agent from being overly reliant on feedback?

The agent must learn to ask for help in a timely way that maximizes the feedback’s informativity while minimizing inconvenience (i.e. annotation cost) to the teacher. In addition, it is important to account for the possibility that a teacher is not always present to improve the generalizability of our setup to real-world settings. Hence, we need to ensure that the agent is not overly reliant on feedback and can still perform well when external help is unavailable. We develop a novel metric to assess the quality of a query and address the considerations above. This is done by calculating the lower bound estimate of the agent’s uncertainty with regards to the task objective and the type of action taken by the agent at each time step.

The main contributions of our proposed learning framework are threefold: 1) We demonstrate the positive effect of teacher-supplied assistance, in the form of image semantic segmentation feedback, on the performance of learning agents. 2) We propose a semi-present teacher training curriculum to train agents that can adapt their behavior to the teacher’s level of availability. 3) We propose a new evaluation metric to assess the quality of the agent’s queries for help.

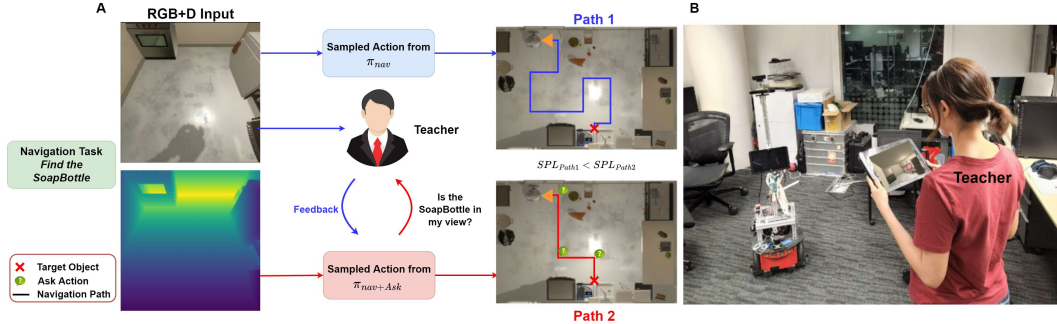


Figure 1: Our learning framework where the agent has an additional capability to ask for feedback during ObjectNav. (A) The overall pipeline of our learning framework and an illustrated comparison in the ObjectNav performance between agents with and without the *ask* action. (B) An illustration of how teacher-learner asking can be accomplished in a real-world setting.

2 Related Work

Object-Goal Navigation [10, 11, 12, 6] has been studied intensively as a fundamental task in the field of embodied AI [8, 9] in recent years. In its simplest form, ObjectNav is the task of navigating to an object, specified by its label, in photorealistic 3D environments [7, 13, 14]. ObjectNav requires the effective combination of multiple capabilities, such as computer vision, navigation and semantic understanding, for good performance. Existing learning-based methods predominantly rely on reinforcement learning (RL) since ObjectNav is a sequential decision-making problem and can naturally be modeled as a Markov decision process (MDP). Learning-based methods for tackling ObjectNav are generally characterized by differences in multiple parts of the RL framework, such as the complexity of their memory architectures (e.g. gated recurrent units [15] and semantic maps [16]) and the amount of prior exploration of the environment [17]. In this work, we focus on making key modifications to the baseline proximal policy optimization (PPO) [18] algorithm.

Interactive Reinforcement Learning [19, 20] accounts for human advice [21, 22, 23], such as guidance and feedback [24], in RL. IRL adopts a human-in-the-loop [25] approach to integrate contextual human knowledge that improves and/or personalizes the behavior of AI agents, depending on the state of the agents. Specifically, human advice during IRL can be used to influence the AI agent’s exploration [17] such that it avoids navigating to states that do not correspond to an optimal policy. This helps to reduce the notorious issue of sample inefficiency in RL [26]. The incorporation of human advice into RL is commonly done through reward shaping [21, 20]. An alternative approach is to treat human advice as input observations for the RL agent’s policy (e.g. gestures in Ges-THOR [27] and state descriptions [28]). Lastly, human advice can be expressed in diverse ways (e.g. language, gesture [27] and image) [19, 28]. In this work, we focus on human feedback in the form of image semantic segmentation, which is then used as observations by the agent. Compared to previous work, this type of human feedback is less costly as it does not require the teacher to be physically next to the agent and does not require privileged environment knowledge.

Active Learning attempts to maximize an agent’s task performance while minimizing the amount of samples annotated [29, 30]. For our ObjectNav task, we aim to minimize the AI agent’s requests for human advice (i.e. human annotation), since each request incurs annotation cost for the person involved, while maximizing the agent’s navigation performance. In general, there are rule-based and neural-based approaches for active learning in IRL. In rule-based approaches, pre-defined heuristics are used to determine when to ask for the human’s help. For example, in the model-confusion method, the agent asks for guidance of the best next action in vision-and-language navigation [31] with a threshold for the difference in action probabilities of the top two actions in its policy [32].

In neural-based approaches, the agent is trained and learns when to ask for help [32, 33]. This generally constitutes expanding the action space in a policy. Previous work has found neural-based approaches to be more robust than rule-based ones [32]. Here, we use a neural-based approach and expand the action space in our agent’s policy to accommodate the *ask* action for the ObjectNav task.

3 Methods

3.1 Problem Formulation

In this work, we tackle the ObjectNav task [11]. To complete the task, the agent must navigate to the target object instance with stopping distance $\leq 1.0\text{m}$, and then issue a termination (i.e., *stop*) action in the proximity of the target object. The object must be within the agent’s field of view in order to succeed. An episode is terminated if the agent issues a termination action, regardless of whether it has succeeded, or if the maximum allowed time step (which is 500 in our setup) is reached. An object is selected at random as the target; we ensure that the agent can reach the target. Placements of objects are randomized every episode. There is only one instance of the target object type in every episode. There are 7 object categories available for all scenes. However, only 5 objects (apple, bowl, potato, soap bottle, and dish sponge) are used in training while we reserve 2 objects (cup and bread) for unseen object test scenarios.

There are many photorealistic embodied AI simulators [7, 14, 13] for indoor navigation tasks. We choose AI2-THOR as our learning environment to train and evaluate our embodied agent because it has diverse scenes and interactive features. AI2-THOR has been widely used for different visual navigation tasks [34, 10]. It also allows the possibility of deploying our learning framework into a real-world robot via RoboTHOR [35]. We use 10 kitchen scenes for training and 5 kitchen scenes for testing. Each scene has its own unique appearance and arrangement. We run each training experiment for 10 million steps and evaluate the agent for 100 episodes on each scene.

The learning agent is represented by a capsule-shaped robot character in AI2-THOR. The agent has six available navigation actions: [*rotate left*, *rotate right*, *move forward*, *look up*, *look down*, and *stop*]. In setups where the feedback mechanism is enabled, the agent has an additional action: [*ask*]. Each rotation action results in a rotation of 90° ; each look up or down action results in an increment or decrement of 30° in the agent’s view angle; the forward action results in a forward displacement of 0.25m . The agent is initialized at a fixed location in a scene.

3.2 Model Architecture

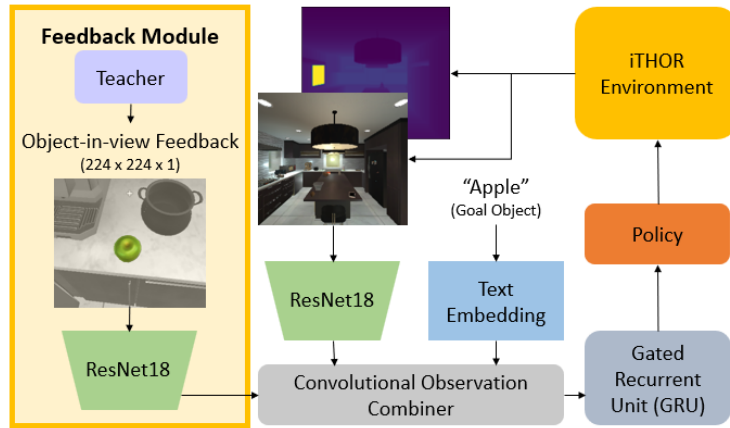


Figure 2: Overall architecture used to learn ObjectNav with the example of a target object “Apple”. The highlighted feedback module on the left is not present in the baseline model.

Figure 2 shows an overview of the model architecture used for our experiments. Like most embodied AI works, we equip our agent with a RGB-D sensor. These visual observations are encoded with pretrained ResNet-18 models [36]. The target object is encoded into a text embedding. In addition to

these classic observations, we provide an **object-in-view observation** that is provided upon each *ask* action, containing the ground truth semantic segmentation observation of the target object’s location in the agent’s view. Pixels which correspond to the target object’s location have a value of 1, and 0 otherwise. The combined observations are passed into a gated recurrent unit (GRU) [37] before the RL model.

We formulate our ObjectNav learning framework using deep RL, specifically an on-policy actor-critic reinforcement learning algorithm - PPO. The actor-critic model has a shared backbone consisting a 2-layer network, with each layer having 256 nodes and ReLU activation. From this last layer, linear prediction heads are used to obtain the value estimate and action distribution. The learning process can be viewed as a MDP. At each time step t , the agent perceives a state s_t from a combination of its sensory and feedback inputs, receives a reward r_t from the environment, and chooses an action a_t according to the current policy π : $a_t \sim \pi_\theta(a_t|s_t)$ where θ represents parameters for the function approximator of the policy π . This action is then executed in the AI2-THOR environment. We implement PPO with a time horizon of 128 steps, batch size of 128, discount factor of 0.99, 4 epochs for each iteration of gradient descent, and buffer size of 2048 for each policy update. We use Adam [38] as the optimizer with a learning rate of $3e-4$. The agent receives a positive reward of +10 if it completes the navigation successfully. To encourage the agent to reach the target object with a minimal amount of steps, the agent receives a small penalty of -0.01 for each time step. AllenAct [9, 39] is used as the codebase for our framework.

3.3 Training Curriculum with Semi-Present Teacher

While our agent is equipped to ask for help, the teacher may not always be present to provide assistance in a real-world setting. In the case where the teacher is absent and help is unavailable, the desired behavior for the agent in this task would be to navigate the scene effectively and autonomously to find the target object, even if it takes more time than asking for feedback. At the same time, the agent should make use of the teacher’s presence with optimal timing to perform its task more efficiently with minimal costs to the teacher.

Hence, we introduce a training curriculum of having a semi-present teacher to improve the agent’s robustness in both settings. We compare between two training curricula: 25% and 75% semi-present teacher. A $\eta\%$ semi-present teacher is present in $\eta\%$ of training episodes. We provide the agent with an additional observation of whether the teacher is present. Feedback is only available to the agent when the teacher is present.

3.4 Quantifying Uncertainty

We propose a metric to quantify the agent’s uncertainty of where the goal is, which is the target object in this case. This metric is also used to quantitatively assess the impact of the *ask* actions.

In a scene s , let $P_s \subseteq \langle \mathbb{N} \times \mathbb{N} \times \mathbb{N} \rangle$ be the set of all possible 3D positions of where the target object can be. At every time step i , we let the likelihood of the target object being at each point $p \in P_s$ be in the range $[0, 1]$. The target object is definitely not at point p if it has a likelihood of 0. We define $\Phi_{s,i} \subseteq P_s \times \mathbb{R}_{[0,1]}$ as the mapping of each possible position to its likelihood in scene s at time step i . Then, the lower bound estimate of the agent’s uncertainty of where the goal is:

$$\lambda_{s,i} = \sum_{p \in P_s} \Phi_{s,i,p} - \max_{p \in P_s} \Phi_{s,i,p} \quad (1)$$

We choose to subtract the maximum value of likelihood in the mapping $\Phi_{s,i}$ so as to ensure that when there is only one position with positive likelihood value, the overall uncertainty $\lambda_{s,i}$ is 0. Beginning at time step $i = 0$, all possible points have equal likelihood of being where the target object is: $\forall p \in P_s : \Phi_{s,0,p} = 1$. It is noted that different scenes in AI2-THOR have different areas, and hence different starting overall uncertainty $\lambda_{s,0}$. We believe that this property realistically reflects the amount of uncertainty in real life, whereby an agent would have a bigger search space if the scene is larger and vice versa.

3.4.1 Uncertainty Change from Navigation

At each time step i , if the action taken is a navigation action that is not a termination (i.e. *rotate left/right*, *move forward* or *look up/down*), then the additional observations that the agent can use

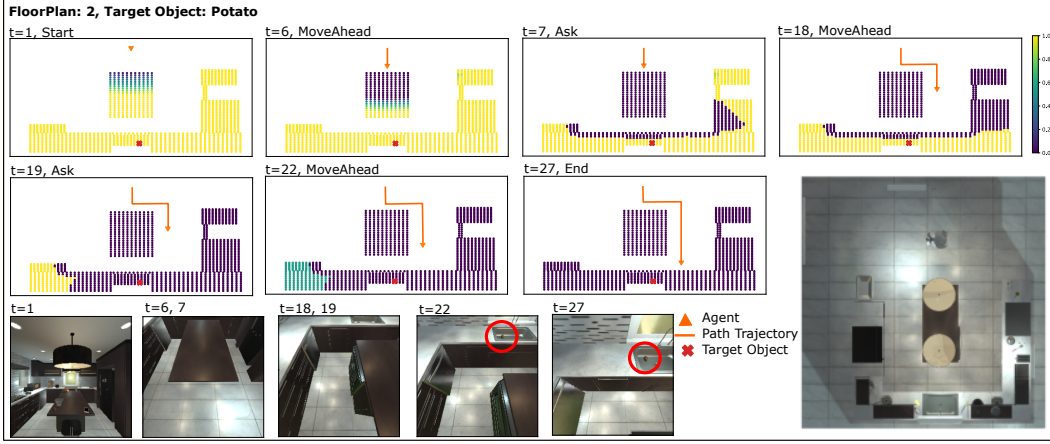


Figure 3: Example of a qualitative result for how the lower bound estimate of the agent’s uncertainty of where the target object is changes for navigation and ask actions: (top) rendering of the uncertainty mapping; (bottom) egocentric RGB observations at the corresponding time steps with the observable target object circled in red; (bottom-right) allocentric view of the scene.

to decrease its uncertainty of target location are RGB and depth. We formulate the decrease of uncertainty from this observation in two cases: when the target object is in view, and when it is not.

When the target object is not in the agent’s view, the change in likelihood mapping is given by:

$$\forall p \in P_s : \Phi_{s,i,p} = \Phi_{s,i-1,p} - \psi(p) \times in(obs_{view}, p) \quad (2)$$

where $in(obs_{view}, p) = 1$ if point p is in the agent’s view else 0, and ψ is a piece-wise linear decay function:

$$\psi(p) = \begin{cases} 1 & \text{if } dist_p \leq \alpha, \\ 1 - \frac{dist_p - \alpha}{\beta - \alpha} & \text{if } dist_p \leq \beta, \\ 0 & \text{otherwise.} \end{cases} \quad (3)$$

where $dist_p$ is the distance from the agent to the point p , and α and β are pre-determined parameters. In our analysis, we define $\alpha = 1.0$ and $\beta = 2.0$, which are respectively $1\times$ and $2\times$ of the proximity distance which the agent has to be of the target object in order to succeed. The decay function is used to mimic the effect that object recognition is often better when the agent is closer to the object. For example, while an agent may mistake a tomato for an apple when it is far away from the object, it would be able to distinguish between the two when it is closer and the visual details are clearer. In Equation 2, the likelihood decreases for every point seen by the agent. This coincides with the agent’s potential gain in knowledge that the target object is not at the seen region.

Suppose that the target object is at position \hat{p} , then when the point \hat{p} is in the agent’s RGB-D view, the change in likelihood mapping is given by:

$$\forall p \in P_s : \Phi'_{s,i,p} = \Phi_{s,i-1,p} - not_is_target(p) \times \psi(p) \times in(obs_{view}, p) \quad (4)$$

and

$$\forall p \in P_s : \Phi_{s,i,p} = \Phi'_{s,i,p} - not_is_target(p) \times \psi(\hat{p}) \quad (5)$$

where

$$is_target(p) = \begin{cases} 1 & \text{if point } p \text{ is where the target object is,} \\ 0 & \text{otherwise.} \end{cases} \quad (6)$$

In Equation 4, the likelihood decreases for every point seen by the agent that does not have the target object. This reflects the agent’s potential gain in knowledge that the target object is not at the seen region. In Equation 5, the likelihood decreases for every point that does not have the target object, including the points not covered by the agent’s view. This is because the target object is in the agent’s view, and Equation 5 reflects the potential gain in knowledge that the target object is less likely to be at other positions.

3.4.2 Uncertainty Change from Feedback

At each time step i , if the action taken is an *ask* action, then the additional observation that the agent can use to decrease its uncertainty of the target object’s location is the object-in-view feedback. We formulate the decrease of uncertainty from this observation in two cases: when the target object is in view, and when it is not.

When the target object is not in the agent’s view, the change in likelihood mapping is given by:

$$\forall p \in P_s : \Phi_{s,i,p} = \Phi_{s,i-1,p} - in(obs_{view}, p) \quad (7)$$

As the object-in-view feedback is a ground truth observation, there is no ambiguity in it. Hence, Equation 7 reflects the potential gain in knowledge that the points in the agent’s view do not contain the target object. On the other hand, if the target object is at position \hat{p} and the point \hat{p} is in the agent’s view, the change in likelihood mapping is given by:

$$\forall p \in P_s : \Phi_{s,i,p} = \Phi_{s,i-1,p} - in(obs_{view}, p) \times not_is_target(p) \quad (8)$$

$$- not_in(obs_{view}, p) \times \psi(\hat{p}) \quad (9)$$

Firstly, Equation 8 reflects the potential gain in knowledge that the points in the agent’s view with non-positive feedback (i.e. object-in-view feedback at that view point is zero) do not contain the target object. Then, the likelihood decreases for all points not covered by the agent’s view. This is because the target object is in the agent’s view, and Equation 8 reflects the potential gain in knowledge that the target object is less likely to be at other positions.

Although object-in-view feedback is a ground truth observation, we still use the decay function with respect to the target object position $\psi(\hat{p})$ in Equation 9 when decreasing the likelihood of other positions not in view. This is to reflect the behaviour where the agent may forget where the target position is if it is far away, and that there may not be a direct route to the target location.

4 Experimental Results

4.1 Evaluation Metrics

We evaluate our agent on these standard navigation metrics [11]: (1) **Success rate (SR)**, the ratio of successful episodes over completed episodes N : $SR = \frac{1}{N} \sum_{i=1}^N S_i$. (2) **Success weighted by path length (SPL)** [4], a measurement of the efficacy of navigation, given by: $SPL = \frac{1}{N} \sum_{i=1}^N S_i \times (\frac{l_i}{max(p_i, l_i)})$ where l_i is the shortest path distance from the agent’s starting position to the goal in episode i , and p_i is the actual path length taken by the agent. Additionally, we propose these new evaluation metrics to justify the effectiveness of the human-agent interaction:

- The percentage of actions taken that are *ask* actions - This metric shows how frequently the agent is asking for feedback.
- The average decrease in uncertainty the target object’s location from *ask* actions - Using the definition of uncertainty and its calculation in Section 3.4, we can quantify how much these *ask* actions are helping the agent in the ObjectNav task.

In the real world, there is no obvious property that is used to quantify when is a good time to ask. However, in this controlled simulated environment, there are instances where we can point out that it is not the most informative time to ask. Hence, in our analysis, we give statistics on the following types of *ask* actions taken: (1) Consecutive *ask* actions: The agent does not gain any new observations or feedback from what it has already received in the previous time steps. (2) Vapid *ask* actions: Ask actions taken when the agent should already have a good idea of where the goal is (i.e. the lower bound estimate of uncertainty is $< 10\%$ of its starting uncertainty). (3) Statistically insignificant *ask* actions: Ask actions which only decrease the uncertainty minimally (i.e. the change in lower bound estimate of uncertainty caused by the *ask* action is less than a threshold γ). We choose $\gamma = 2.0$, about 10% of the average decrease in uncertainty by all actions in the baseline.

4.2 Analysis

We use two methods to evaluate the impact of the *ask* action on the agent’s performance: (1) **Baseline**: the agent only has the visual (i.e. RGB and depth images) and object category information. (2)

Teacher Presence	Methods	Success Rate (%)				Success weighted by Path Length (%)			
		Both Seen	Unseen Objects	Unseen Scenes	Both Unseen	Both Seen	Unseen Objects	Unseen Scenes	Both Unseen
False	Baseline	35.2	13.0	18.6	11.9	24.1	6.9	9.1	7.7
False	Semi-25	40.6	13.3	23.1	7.9	26.8	18.5	11.6	4.5
False	Semi-75	33.9	18.5	18.1	6.7	27.4	16.3	11.4	6.7
True	Feedback	70.9	37.0	71.4	26.3	46.4	24.2	39.7	17.2
True	Semi-25	51.6	15.1	35.7	18.6	34.1	8.3	20.2	12.4
True	Semi-75	72.1	24.8	50.1	8.6	50.9	18.9	34.0	4.6

Table 1: Success Rate (SR) and Success weighted by Path Length (SPL) evaluation results for different seen and unseen cases for objects and scenes across methods.

Object-in-view feedback: in addition to (1), the agent receives object-in-view feedback upon asking for help. From Table 1, we see that object-in-view feedback method outperforms the baseline in all cases by an average of 31.7% and 19.9% for SR and SPL respectively. This shows that the agent understands how to use the feedback, i.e. learning the semantic meaning of the given feedback. As expected, the agent’s performance decreases as more parts of the test scenario (i.e. target object and scene) are unseen during training. We can also see that performance deterioration is generally more significant for unseen objects than for unseen scenes and the most significant for test scenarios with simultaneously unseen objects and scenes. In our supplementary material, we present results of the object-in-view feedback expressed as natural language instead of image semantic segmentation.

Table 1 also shows the results from our semi-present teacher training curriculum in Section 3.3. We label Semi- η as the method used to train an agent with $\eta\%$ present teacher curriculum. We discover that the agent trained with object-in-view feedback and a 100% present teacher fails in 95% of all test episodes when the teacher is absent, performing significantly worse than the baseline which has a SR of at least 11.9%. This shows that the agent is over-reliant on the teacher’s feedback with a 100% present teacher training curriculum and cannot generalize well when the teacher is absent. However, both agents trained from the 25% and 75% present teacher curricula achieve comparable performance to that of the baseline’s when the teacher is absent during test scenarios, with a maximum SR decrease of 5.2%. This shows that a simple curriculum of mixing in episodes with no teacher feedback helps the agent learn to react more robustly to the absence of a teacher. The benefits of feedback can be seen as Semi-25 and Semi-75 agents achieve a maximum increase of 38.2% in SR and 23.5% in SPL with the presence of a teacher. We also note that Semi-25 and Semi-75 agents’ performance with a present teacher is not as high as that when trained with an always present teacher with a minimum SR decrease of 7.7%.

Using the uncertainty metric defined in Section 3.4, we present the average decrease in uncertainty caused by navigation or *ask* actions in Table 2. The average uncertainty change by *ask* actions is higher than that by navigation actions for the agent trained with an always present teacher and Semi-75. This shows that the object-in-view feedback received by the agent from *ask* actions is statistically useful in helping the agent complete the task more efficiently. Figure 3 shows a qualitative example of how uncertainty changes in an episode from navigation and *ask* actions.

The agent trained with an always present teacher uses the highest percentage of *ask* actions. Table 3 shows the percentages of the different types of *ask* actions taken across different training curricula. The percentage of consecutive *ask* actions taken by the agent trained with an always present teacher is close to zero, suggesting that the agent is successful in learning that there is no additional gain in information when asking consecutively. Comparing across methods, the agent trained with an always present teacher has the lowest percentage of consecutive *ask* actions, vapid *ask* actions, and statistically insignificant *ask* actions, followed by Semi-75 and lastly Semi-25. This suggests that while the agent trained with an always present teacher uses a higher percentage of *ask* actions, it has learned to utilize them in a statistically informative manner. While the percentages of vapid asks and statistically insignificant asks (as defined in Section 4.1) seem high, this is partly attributed to the way the uncertainty metric is defined. This metric is a lower bound estimate of the agent’s uncertainty of where the goal is. It assumes a perfect memory where uncertainty only decreases with more observations, which may not be the case for an RL agent.

Teacher Presence	Methods	Average change in uncertainty by Nav actions				Average change in uncertainty by Ask actions			
		Both Seen	Unseen Objects	Unseen Scenes	Both Unseen	Both Seen	Unseen Objects	Unseen Scenes	Both Unseen
False	Baseline	13.8	6.8	6.9	2.43	-	-	-	-
False	Semi-25	15.8	26.1	8.1	8.8	-	-	-	-
False	Semi-75	19.5	17.2	13.8	17.8	-	-	-	-
True	Feedback	15.6	17.3	6.7	14.2	22.2	26.4	7.6	21.9
True	Semi-25	20.1	29.4	6.4	6.9	23.6	10.5	15.6	30.8
True	Semi-75	19.4	11.0	11.6	7.0	28.3	13.6	21.2	19.9

Table 2: Average change in agent’s overall uncertainty by navigation and ask actions for different seen and unseen cases for objects and scenes across methods.

Methods	% of Ask actions in all actions				% of Consecutive Ask actions in all ask actions			
	Both Seen	Unseen Objects	Unseen Scenes	Both Unseen	Both Seen	Unseen Objects	Unseen Scenes	Both Unseen
Feedback	34.9	37.4	42.1	24.6	0.3	0.4	0.2	0.4
Semi-25	15.6	12.2	17.1	13.5	14.3	5.8	16.1	11.8
Semi-75	23.1	25.8	19.3	16.2	5.4	5.6	5.5	5.1
Methods	% of Vapid Ask actions in all ask actions				% of Statistically Insignificant Ask actions in all ask actions			
	Both Seen	Unseen Objects	Unseen Scenes	Both Unseen	Both Seen	Unseen Objects	Unseen Scenes	Both Unseen
Feedback	57.8	63.3	70.4	70.8	80.3	73.8	94.2	81.2
Semi-25	86.0	86.2	78.3	88.2	93.6	80.0	96.0	86.3
Semi-75	75.4	64.6	73.4	70.1	78.9	87.9	94.3	83.4

Table 3: Statistics on the types of ask actions taken for different seen and unseen cases across methods where feedback is available. Teacher is present in all episodes used for evaluation here.

5 Conclusion

In this work, we demonstrate the importance of quality feedback signals toward robot learning for the task of object-goal navigation. We propose a learning framework that enables the embodied agent to optimize its navigation policy for ObjectNav tasks by learning to request for feedback. Additionally, we propose a semi-present teacher training curriculum to increase the agent’s robustness when a teacher is not always present. Finally, we develop a formulation of the lower bound estimate of the uncertainty that quantitatively measures the timing and robustness of the learning agent’s feedback-seeking behavior, and show that our framework encourages effective agent behaviors for ObjectNav.

Limitations and future work. (1) Our current framework assumes perfect feedback, which may be unrealistic in a real-world setting. A future direction could be to make the interactive learning framework more robust by providing noisy or imperfect feedback. (2) As a proof of concept, we briefly investigated using natural language as a feedback modal (presented in our supplementary material). Human interaction comes in many modals. For similar semantic meanings in a feedback, future work directions can include the study of modular and exchangeable feedback encoders whereby the algorithm does not need to be retrained for a different feedback modal.

References

- [1] G. N. DeSouza and A. C. Kak. Vision for mobile robot navigation: A survey. *IEEE transactions on pattern analysis and machine intelligence*, 24(2):237–267, 2002.
- [2] M. MacMahon, B. Stankiewicz, and B. Kuipers. Walk the talk: Connecting language, knowledge, and action in route instructions. *Def*, 2(6):4, 2006.
- [3] D. Chen and R. Mooney. Learning to interpret natural language navigation instructions from observations. In *Proceedings of the AAAI Conference on Artificial Intelligence*, volume 25, pages 859–865, 2011.
- [4] P. Anderson, Q. Wu, D. Teney, J. Bruce, M. Johnson, N. Sünderhauf, I. Reid, S. Gould, and A. Van Den Hengel. Vision-and-language navigation: Interpreting visually-grounded navigation instructions in real environments. In *Proceedings of the IEEE conference on computer vision and pattern recognition*, pages 3674–3683, 2018.

- [5] H. Chen, A. Suhr, D. Misra, N. Snavely, and Y. Artzi. Touchdown: Natural language navigation and spatial reasoning in visual street environments. In *Proceedings of the IEEE/CVF Conference on Computer Vision and Pattern Recognition*, pages 12538–12547, 2019.
- [6] S. Y. Gadre, M. Wortsman, G. Ilharco, L. Schmidt, and S. Song. Clip on wheels: Zero-shot object navigation as object localization and exploration. *arXiv preprint arXiv:2203.10421*, 2022.
- [7] E. Kolve, R. Mottaghi, W. Han, E. VanderBilt, L. Weihs, A. Herrasti, D. Gordon, Y. Zhu, A. Gupta, and A. Farhadi. Ai2-thor: An interactive 3d environment for visual ai. *arXiv preprint arXiv:1712.05474*, 2017.
- [8] J. Duan, S. Yu, H. L. Tan, H. Zhu, and C. Tan. A survey of embodied ai: From simulators to research tasks. *IEEE Transactions on Emerging Topics in Computational Intelligence*, 2022.
- [9] L. Weihs, J. Salvador, K. Kotar, U. Jain, K.-H. Zeng, R. Mottaghi, and A. Kembhavi. Allenact: A framework for embodied ai research. *arXiv preprint arXiv:2008.12760*, 2020.
- [10] Y. Zhu, R. Mottaghi, E. Kolve, J. J. Lim, A. Gupta, L. Fei-Fei, and A. Farhadi. Target-driven visual navigation in indoor scenes using deep reinforcement learning. In *2017 IEEE international conference on robotics and automation (ICRA)*, pages 3357–3364. IEEE, 2017.
- [11] D. Batra, A. Gokaslan, A. Kembhavi, O. Maksymets, R. Mottaghi, M. Savva, A. Toshev, and E. Wijmans. Objectnav revisited: On evaluation of embodied agents navigating to objects. *arXiv preprint arXiv:2006.13171*, 2020.
- [12] F. Zhu, Y. Zhu, V. Lee, X. Liang, and X. Chang. Deep learning for embodied vision navigation: A survey. *arXiv preprint arXiv:2108.04097*, 2021.
- [13] M. Savva, A. Kadian, O. Maksymets, Y. Zhao, E. Wijmans, B. Jain, J. Straub, J. Liu, V. Koltun, J. Malik, et al. Habitat: A platform for embodied ai research. In *Proceedings of the IEEE/CVF International Conference on Computer Vision*, pages 9339–9347, 2019.
- [14] C. Li, F. Xia, R. Martín-Martín, M. Lingelbach, S. Srivastava, B. Shen, K. Vainio, C. Gokmen, G. Dharan, T. Jain, et al. Iqibson 2.0: Object-centric simulation for robot learning of everyday household tasks. *arXiv preprint arXiv:2108.03272*, 2021.
- [15] K. Cho, B. Van Merriënboer, D. Bahdanau, and Y. Bengio. On the properties of neural machine translation: Encoder-decoder approaches. *arXiv preprint arXiv:1409.1259*, 2014.
- [16] D. S. Chaplot, D. P. Gandhi, A. Gupta, and R. R. Salakhutdinov. Object goal navigation using goal-oriented semantic exploration. *Advances in Neural Information Processing Systems*, 33: 4247–4258, 2020.
- [17] S. K. Ramakrishnan, D. Jayaraman, and K. Grauman. An exploration of embodied visual exploration. *International Journal of Computer Vision*, 129(5):1616–1649, 2021.
- [18] J. Schulman, F. Wolski, P. Dhariwal, A. Radford, and O. Klimov. Proximal policy optimization algorithms. *arXiv preprint arXiv:1707.06347*, 2017.
- [19] B. Poole and M. Lee. Towards intrinsic interactive reinforcement learning: A survey. *arXiv preprint arXiv:2112.01575*, 2021.
- [20] C. Arzate Cruz and T. Igarashi. A survey on interactive reinforcement learning: design principles and open challenges. In *Proceedings of the 2020 ACM designing interactive systems conference*, pages 1195–1209, 2020.
- [21] R. Zhang, F. Torabi, L. Guan, D. H. Ballard, and P. Stone. Leveraging human guidance for deep reinforcement learning tasks. *arXiv preprint arXiv:1909.09906*, 2019.
- [22] A. Najar and M. Chetouani. Reinforcement learning with human advice: A survey. *Frontiers in Robotics and AI*, 8, 2021. ISSN 2296-9144. doi:10.3389/frobt.2021.584075. URL <https://www.frontiersin.org/article/10.3389/frobt.2021.584075>.

- [23] R. Maclin and J. W. Shavlik. Creating advice-taking reinforcement learners. *Machine Learning*, 22(1):251–281, 1996.
- [24] P. F. Christiano, J. Leike, T. Brown, M. Martic, S. Legg, and D. Amodei. Deep reinforcement learning from human preferences. *Advances in neural information processing systems*, 30, 2017.
- [25] X. Wu, L. Xiao, Y. Sun, J. Zhang, T. Ma, and L. He. A survey of human-in-the-loop for machine learning. *Future Generation Computer Systems*, 2022.
- [26] H. B. Suay and S. Chernova. Effect of human guidance and state space size on interactive reinforcement learning. In *2011 RO-MAN*, pages 1–6, 2011. doi:10.1109/ROMAN.2011.6005223.
- [27] Q. Wu, C.-J. Wu, Y. Zhu, and J. Joo. Communicative learning with natural gestures for embodied navigation agents with human-in-the-scene. In *2021 IEEE/RSJ International Conference on Intelligent Robots and Systems (IROS)*, pages 4095–4102. IEEE, 2021.
- [28] K. Nguyen, Y. Bisk, and H. Daumé III. Learning when and what to ask: a hierarchical reinforcement learning framework. *arXiv preprint arXiv:2110.08258*, 2021.
- [29] P. Ren, Y. Xiao, X. Chang, P.-Y. Huang, Z. Li, B. B. Gupta, X. Chen, and X. Wang. A survey of deep active learning. *ACM Computing Surveys (CSUR)*, 54(9):1–40, 2021.
- [30] C. C. Aggarwal, X. Kong, Q. Gu, J. Han, and S. Y. Philip. Active learning: A survey. In *Data Classification*, pages 599–634. Chapman and Hall/CRC, 2014.
- [31] J. Gu, E. Stefani, Q. Wu, J. Thomason, and X. E. Wang. Vision-and-language navigation: A survey of tasks, methods, and future directions. *arXiv preprint arXiv:2203.12667*, 2022.
- [32] T.-C. Chi, M. Shen, M. Eric, S. Kim, and D. Hakkani-tur. Just ask: An interactive learning framework for vision and language navigation. In *Proceedings of the AAAI Conference on Artificial Intelligence*, volume 34, pages 2459–2466, 2020.
- [33] K. Nguyen and H. Daumé III. Help, anna! visual navigation with natural multimodal assistance via retrospective curiosity-encouraging imitation learning. *arXiv preprint arXiv:1909.01871*, 2019.
- [34] W. Yang, X. Wang, A. Farhadi, A. Gupta, and R. Mottaghi. Visual semantic navigation using scene priors. *arXiv preprint arXiv:1810.06543*, 2018.
- [35] M. Deitke, W. Han, A. Herrasti, A. Kembhavi, E. Kolve, R. Mottaghi, J. Salvador, D. Schwenk, E. VanderBilt, M. Wallingford, L. Weihs, M. Yatskar, and A. Farhadi. Robothor: An open simulation-to-real embodied ai platform. In *IEEE/CVF Conference on Computer Vision and Pattern Recognition (CVPR)*, June 2020.
- [36] K. He, X. Zhang, S. Ren, and J. Sun. Deep residual learning for image recognition. In *2016 IEEE Conference on Computer Vision and Pattern Recognition (CVPR)*, pages 770–778, 2016. doi:10.1109/CVPR.2016.90.
- [37] R. Dey and F. M. Salem. Gate-variants of gated recurrent unit (gru) neural networks. In *2017 IEEE 60th International Midwest Symposium on Circuits and Systems (MWSCAS)*, pages 1597–1600, 2017. doi:10.1109/MWSCAS.2017.8053243.
- [38] D. Kingma and J. Ba. Adam: A method for stochastic optimization. *International Conference on Learning Representations*, 12 2014.
- [39] E. Wijmans, A. Kadian, A. Morcos, S. Lee, I. Essa, D. Parikh, M. Savva, and D. Batra. Dd-ppo: Learning near-perfect pointgoal navigators from 2.5 billion frames. *arXiv preprint arXiv:1911.00357*, 2019.